Towards in-cell structural study of light-harvesting complexes : an investigation with MAS-NMR

Azadi Chegeni, F.

CHAPTER 1

Introduction & Methodological background

General introduction

Current energy resources, fossil fuels, make that mankind faces a number of challenges including finite resources that will eventually dwindle, rising prices and environmental damages such as global warming and air pollution. In this light, development of renewable energy sources has drawn much attention in recent years.

As long as the sun is shining, solar energy reaching the earth is the cleanest source of renewable energy. Over the last decades a wide array of techniques such as photovoltaic cells have been developed to harvest the sunlight and convert it to power. However, nature has developed an efficient way of harnessing the solar energy for billions of years. Photosynthesis is the primary process that sustains the vast majority of life on earth. Photosynthetic organisms convert light energy through a complicated series of events into biochemical energy. For decades, researchers have been trying to improve this fundamental process and many biophysical and molecular biological techniques have been employed to characterize and manipulate different elements of photosynthetic organisms. Recent advances in photosynthesis research at the molecular level promise new routes for increasing biomass production [1].

Harvesting light is the first step in the process of solar energy conversion that is carried out by antenna complexes of all photosynthetic organisms. Light harvesting antennas of plants and algae are flexible, which enable them to adapt to light fluctuations avoiding photodamages. Their antennas can switch into a photoprotective state that dissipates the incoming sunlight, which protects against light stress but reduces photosynthetic efficiency. To date, by combination of several spectroscopic methods and high resolution crystallography, our understanding of regulation of light harvesting has improved. However, due to the lack of an atomistic insight into the conformational dynamics of antenna complexes there are yet many questions concerning the molecular mechanisms of photo protection that have remained unanswered.

This thesis applies solid-state nuclear magnetic resonance (NMR) spectroscopy as an emerging technique for *in-situ* characterization of the conformational dynamics of photosynthetic light-harvesting complexes at atomistic level. Furthermore, this study paves the way for the use of solid state NMR for *in-situ* and *in-cell* detection of molecular dynamics of photosynthetic membrane constituents.

Chlamydomonas reinhardtii

Microalgae are a group of eukaryotic photosynthetic organisms that recently attract a widespread attention for new generation of biofuels. *Chlamydomonas reinhardtii* (*Cr.*) is an ancient unicellular microalgae which has occupied the earth fresh water and soil over one billion years. High adaptability of *Cr.* to different conditions makes it a unique model system for research on many fundamental questions of photosynthesis. Manipulation of *Cr.* genes is relatively easy and the cells grow quickly in organic carbon sources under controlled environmental conditions while maintaining the function of the photosynthetic apparatus. *Cr.* cells are about 10 micrometers long and have two flagella's for mobility, several mitochondria, a single chloroplast that photosynthetic apparatus reside in, a cell wall made of glycoproteins and an eye spot to sense light direction and intensity [2]. A schematic picture of a *Chlamydomonas* cell is presented in figure 1.

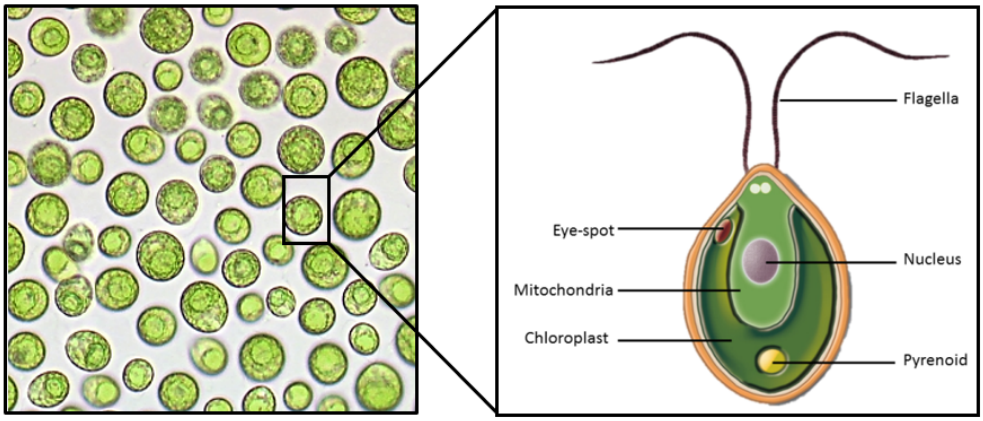

Figure 1. *Chlamydomonas reinhardtii* cell illustration (www.pt.pngtree.com).

Thylakoid membrane architecture

Oxygenic photosynthesis is the process by which plants, algae and cyanobacteria use solar energy to synthesis biomass from carbon dioxide and produce oxygen as a waste product. The processes of oxygenic photosynthesis evolved approximately 2.5 billion years ago and produce all the oxygen on earth. The general reaction of oxygenic photosynthesis can be indicated by the following simplified equation:

$$carbon\ dioxide + water \xrightarrow{sunlight} sugar + oxygen$$

All components of the photosynthetic apparatus that are necessary for the photosynthesis reside in the chloroplast of plant and algae, in cylindrical shaped sheets known as thylakoid membranes. Thylakoid membranes are differentiated into two membrane domains, the cylindrical stacked structures known as grana and the single-membrane regions called stroma lamellae (see figure 2).

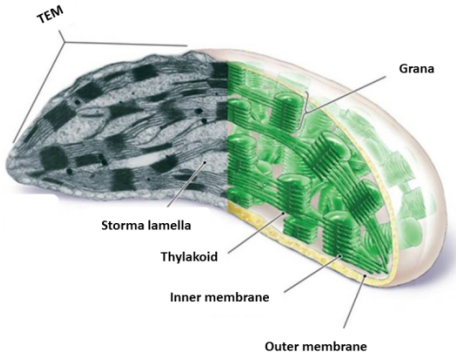

Figure 2. Schematic illustration of a chloroplast (www.biologyexams4u.com).

Photosynthesis takes place in two stages. In the light reactions, solar energy is harvested and stored in the form of ATP and NADPH and oxygen is released as a byproduct. In the dark reaction, ATP and NADPH drive sugar synthesis. There are four main membrane complexes that drive the light reaction in thylakoids: antenna-photosystem II (PSII-LHCII) and antenna-photosystem I (PSI-LHCI) protein-pigment super-complexes, cytochrome-b_6f complex (Cyt b_6f) and ATP-synthase complex. Figure 3 presents a schematic view of the electron transport through the thylakoid membrane. The process starts with light harvesting complexes of PSII, where light energy is absorbed by chlorophyll molecules and transferred via a series of carriers to the reaction center of PSII to induce the excitation of a special pair of chlorophylls (P680 to P680*). This creates a charge-separated state and the electron is transferred on to the chain of electron carriers. The $P680^+$ now is a potential electron acceptor and takes up an electron extracted from water, while protons are released to the thylakoid lumen. At this stage oxygen is produced as a byproduct. The electron is first transferred to a plastoquinone (PQ) in the PSII and after two turnovers, PQ is fully reduced to plastoquinol (PQH_2). The plastoquinol then diffuses into the thylakoid membrane. Via the plastoquinol, electrons are transferred to Cyt b_6f and then to plastocyanin via a cycle of reactions (Q-cycle) and finally to PSI. Similarly to PSII, harvested

solar energy is transferred to the reaction center of PSI and excites the special pair of chlorophylls, P700, to P700*. A charge-separated state is created in P700 and the transferred electron reduces the protein ferredoxin in the stroma and from the ferredoxin, electrons are finally stabilized by reduction of $NADP^+$ to NADPH. The electrons from plastocyanin are used to reduce the $P700^+$. During the electron transfer process, protons are also released into the thylakoid lumen. Finally, charge separation and electron transfer in thylakoid membranes lead to formation of a proton gradient which is used to drive ATP-synthase and produce ATP. The last stage of photosynthesis occurs in the dark via the Calvin-cycle in which the generated ATP and NADPH is used to convert CO_2 to carbohydrates [3].

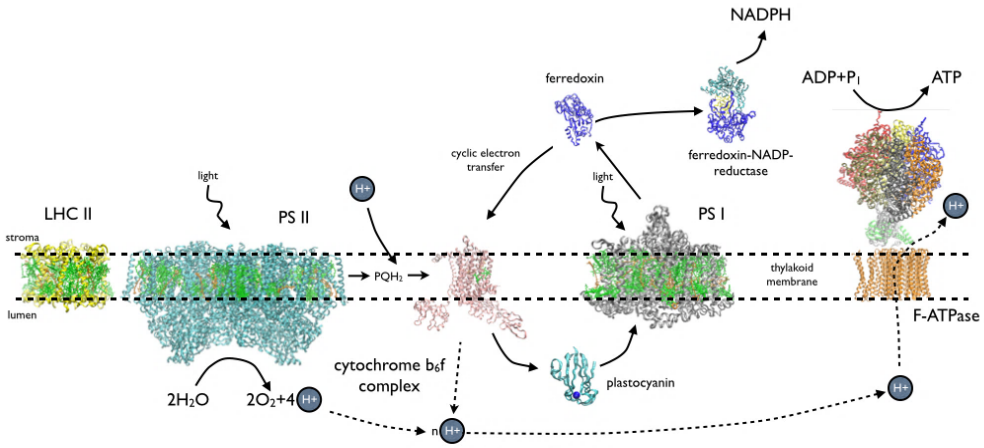

Figure 3. Process of photosynthesis in the thylakoid membrane and major protein complexes involved.

Light-harvesting complexes

In higher plants and algae, PSI-LHCI and PSII-LHCII super complexes consist of two parts: a core complex that contains all the cofactors of the electron transport chain, and the outer antenna complexes (LHCs) to capture light energy and transfer excitation to the reaction center [4-5]. Considerable effort has been made to isolate PSI and PSII from a wide range of organisms in order to get more insight into their molecular structure and function.

The available X-ray structure of PSI from cyanobacteria at 2.5 Å provides the location of the individual subunits and cofactors together with information on protein-cofactor interactions. According to the X-ray structure, PSI forms as a trimer and the core complex of PSI is composed of 14 protein subunits binding 90 chlorophyll *a* (Chl *a*) and 22 carotenoids (Car) [6]. The outer antenna, known as light-harvesting complex I (LHCI), encoded by 4 genes (Lhc1-4) and also

coordinates cofactors [4, 7]. Although the core complex of PSI in cyanobacteria, higher plants and green algae is highly conserved [8-12], the outer antenna (LHCI) of *Chlamydomonas reinhardtii* (*Cr.*) shows a significant difference in the number of genes that encode for the LHC polypeptides [13-14]. LHCI of *Cr.* is composed of nine Lhca proteins (Lhca1–9) with different spectroscopic properties, located on one side of the core in a double half ring arrangement [15]. However the light harvesting complex of PSI in higher plants consists of 4 (Lhca1-4) genes on one side of the core in the form of a single half ring [16].

Several atomic structures of PSII are also available with resolutions ranging from 3.8 to 1.9 Å [17-19] and recently a high-resolution cryo-EM structure of a spinach PSII-LHCII supercomplex at 3.2 Å has become available [20] (see figure 4). According to the X-ray and cryo-EM structures, several major LHCII trimers and a few minor monomer antennas are associated with the two sides of dimeric PSII. Similar to PSI, the core complex of PSII is also conserved between different photosynthetic organisms [5]. In higher plants, the outer antenna of PSII is composed of three Lhcb (Lhcb1-3) genes which encode the major trimeric antenna complexes and three genes (Lhcb4-6) forming the minor antennas. Minor antennas of PSII form as monomers and depend on their molecular weight are differentiated as CP29, CP26 and CP24. In *Cr.* nine different genes (Lhcbm1-9) encode the protein polypeptides. CP24 minor antenna is lacking in the genome of *Cr.* algae while CP29 and CP26 are present. The LHCII trimers consist of isomers and the pigment binding sites are conserved among all sequences. However, different polypeptides have specialized roles in photoprotection, for example, among the most abundant polypeptides, Lhcbm1 is involved in excess energy dissipation [21], whereas Lhcbm2 and Lhcbm7 are essential for state transitions where LHCII dislocate from PSII to PSI in order to reduce the light stress on PSII [22].

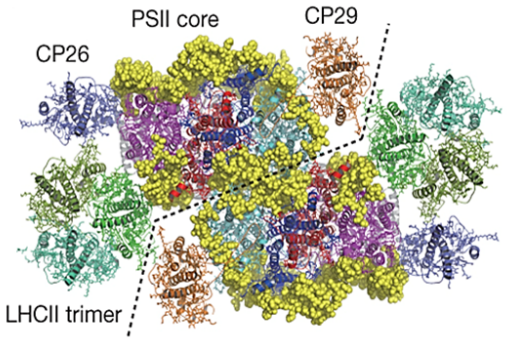

Figure 4. Top view of LHCII-PSII supercomplex resolved at 3.2 Å by cryo-electron microscopy [20].

Light harvesting complex II (LHCII)

Extensive efforts have been made to uncover the molecular structure of the major antenna complex LHCII. The first structure of LHCII from pea has been determined by electron crystallography at 3.4 Å resolution [23]. This model revealed three transmembrane α-helices (helices A, B and C) and a short helix (helix D), 12 chlorophylls and two carotenoids. A more detailed structural picture of LHCII is essential to have a better understanding of the functional mechanism of LHCII. High-resolution X-ray crystallography provided a more detailed structure of protein and cofactors at 2.5 Å [24]. Each LHCII monomeric structure is characterized by three membrane-spanning helices (helix A-C) and two short helical fragments (helix D and E), an N-terminal stretch and C-tail, and segments containing large, water-exposed loops. Figure 5 (A-C) shows the (Lhcb1 based) monomeric protein structure of LHCII, the pigment-protein structure, and a top view of the trimeric structure of LHCII. Each monomer subunit binds many pigments including 8 Chl *a*, 6 Chl *b*, 2 lutein, neoxanthin and one xanthophyll-cycle carotenoid. Six Chls are close to the lumenal side of the membrane, while the remaining chlorophylls are close to the stromal side. The binding of the Chls to the proteins involves amino acid side chains or backbones that coordinate the central Mg of the Chls. In addition, water molecules and lipids are involved in the binding of chlorophylls. The orientation of the pigments with respect to each other in the LHCII complex is presented in figure 6.

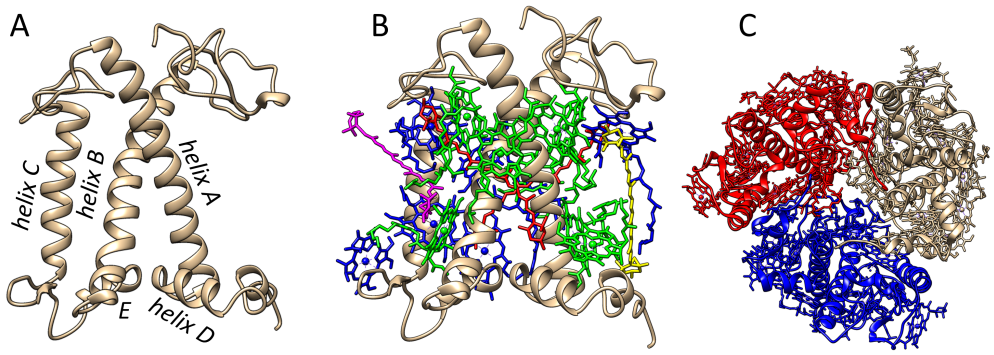

Figure 5. **A:** LHCII protein structure, **B:** LHCII structure including the pigments, **C:** top view of a trimeric LHCII complex.

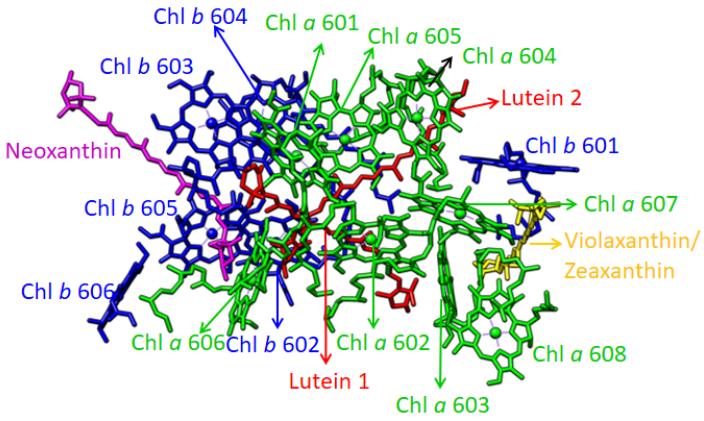

Figure 6. Orientation and numbering of pigments in each monomeric LHCII according to the crystal structure of LHCII spinach (*2bhw*). Chl *a* molecules are presented in green, Chl *b* in blue, lutein in red, neoxanthin in purple and violaxanthin/zeaxanthin in yellow.

Photo-protection

Although light is essential for growth of photosynthetic organisms, fluctuation in light intensity could lead to over-excitation of the photosystems, resulting in photo oxidative damage. In excess light, plant and algae can regulate light harvesting using different photo protective mechanisms such as rearranging the light harvesting complexes, thermally dissipating excess light energy and altering electron transport [25].

Photoprotective processes are highly regulated by thylakoid membrane responses, the conformational flexibility of proteins, as well as the interplay of the complexes within a dynamic thylakoid membrane environment [26-27]. In particular, light-harvesting antenna complexes (LHCs) can adapt to light harvesting, or form dissipative photo protective states as a mechanism to regulate photosynthesis under light stress. The photo-protective feedback response is activated by acidification of the thylakoid luminal environment as a result of over-excitation in a process called non-photochemical quenching (NPQ) [28]. Photo-protection and NPQ have a major influence for photosynthetic productivity and it was recently demonstrated that manipulation of the photo protective response could give a remarkable 15-20% increase of biomass yields in the field [1].

So far numerous efforts have been made to understand the photo-protective mechanisms performed by photosynthetic organisms. Depending on the time scale of the induction and relaxation four types of NPQ processes can be

distinguished: energy dependent quenching (qE) [29], state transition dependent quenching (qT) [30], Zeaxanthin (Zea) dependent quenching (qZ) [31] and photo inhibitory quenching (qI) [32] see figure 7. Different NPQ processes are briefly explained as follows:

Due to the photo-induced damage of the reaction center in PSII, the energy conversion efficiency and photosynthesis capacity is reduced by photosynthetic organisms. This process is known as photoinhibition or qI. qI, the slowest NPQ process, is a reversible process and it is responsible for long, continuous thermal dissipation of excitations that might take hours [33]. qZ is induced on a time scale of minutes and it is related to the acidification of the thylakoid lumen under high light stress, which activates violaxanthin (Vio) de-epoxidase enzymes (VDE) that convert Vio to Zea via the reversible xanthophyll cycle [3]. The exact role of Zea is still under debate, However, it has been shown that zea enhances the NPQ in the thylakoid membrane [34]. qT involves the phosphorylation of LHCII antenna complexes and reversible membrane state transitions where LHCII complexes detach from PSII and associate with PSI to balance the activity of PSII and PSI and reduce the light stress on PSII. This process is also induced within minutes [30]. The last NPQ component, qE, is the most rapid component of NPQ that is believed to dissipate the excess light energy by reducing the excited-state life times of the antenna chlorophylls, preventing the thylakoid membrane from over-excitation. qE is activated upon lumen acidification via a pH-sensing protein-pigment complex known as LHCSR in algae and PsbS in plants. qE also prevents the over reduction of electron carriers in the plastoquinone by decreasing the rate of singlet oxygen formation [29].

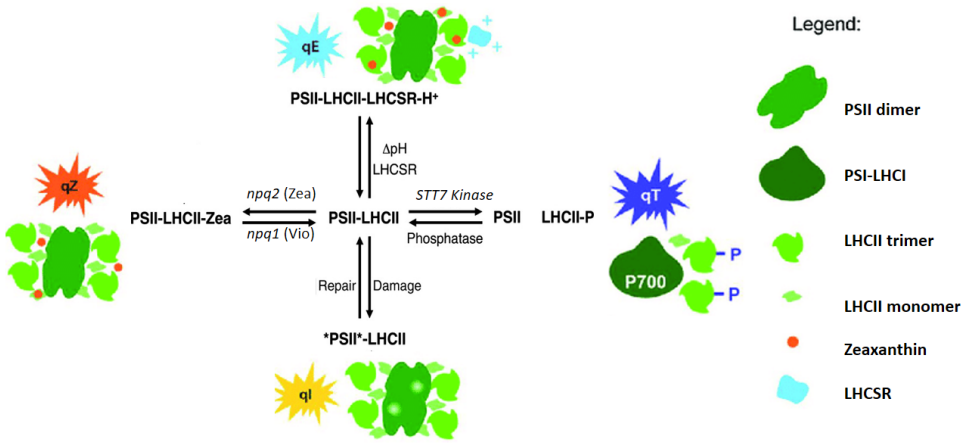

Figure 7. Schematic illustration of non-photochemical quenching in *Chlamydomonas reinhardtii* (*Cr.*) adapted from [25, 35] (Erikson 2015 and Malnoe 2018).

It is widely believed that the quenching mechanism is also active at the level of isolated light harvesting complexes and several quenching sites have been proposed [25, 35]. However the conformational changes associated with the quenching switch of the light harvesting complexes were not resolved.

pH-sensitive proteins like PsbS and LHCSR in plants and algae are suggested to play a role in inducing NPQ by protonation of their pH-sensing domains in membranes and isolated complexes [36-38]. Protonation of the pH-sensor proteins promotes a conformational switch of the antenna to a quenched state. The effect of Zea in quenching has been investigated extensively in plants and green algae and it has been proposed that Zea might be a direct quencher of excitations forming charge-transfer states [39]. Accumulation of Zea at the membrane level was also suggested to protect polyunsatured lipids during light stress [40]. According to Horton & Ruban *et al*, Zea might have an allosteric effect owing to its hydrophobicity compared with Vio [41]. It might promote a conformational change in LHCs that stabilizes the quenched state in combination with low pH [42]. However Croce *et al,* showed that just the effect of Zea binding and low pH is not enough to create a quenched state and they propose that the important role of Zea lies in its location at the interfaces between complexes [34]. Moreover, based on the Chl-Car interactions, different quenching sites regarding the mechanism of quenching have been proposed [43-47].

Up to date, various methods have been introduced to understand the molecular mechanisms that regulate photosynthesis. However until now, no structure-based methods have been presented that could provide a direct view of different photosynthetic molecular components inside the native membrane environments. Solid-state NMR spectroscopy has shown to be a powerful tool for atomistic detection of different molecular sites of membrane proteins even in native membranes or cellular environments [48-58]. Application of solid state NMR to photosynthetic systems and a methodological background of the method, which have been used in this thesis are discussed in the following sections.

Application of solid-state NMR in photosynthesis research

During the past decades, X-ray crystallography has been the major technique to resolve the structure of photosynthetic membrane proteins [59-60]. However, detecting the atomistic details of structure-function interaction in flexible environments remains a daunting task [61]. Solid state NMR has become rapidly an emerging technique for atomistic detection of the structure and dynamics of photosynthetic membrane proteins.

Solid-state NMR spectroscopy has contributed to enhance the understanding of light harvesting, charge separation and photo protection in photosynthesis. A sequence specific assignment of protein sites has been obtained for light harvesting complex 2 of *Rhodopseudomonas acidophila* (LH2) providing the secondary structure to complement the crystallographic data. Later on, solid state NMR provided an accurate prediction of pigment electronic structures in the ground state of *Rhodospirillum Acidophila* LH1 and LH2 [58]. The structural and functional properties of heterogeneous chlorosome antenna of green bacteria were studied by solid state NMR and cryo-EM, introducing a model system for self-assembled artificial antenna [62-63]. Solid state NMR studies on LHCII demonstrated that the LHCII conformational switch involves rearrangements of the Arg residue in the stromal loop [64] and the LHCII switch into a photo-protective state is accompanied by changes in the Chl *a* ground-state electronic structures [65] which were explained by altered Chl-lutein interactions [66].

Furthermore, the photo-chemical induced nuclear polarization (photo-CIDNP) effect has been observed for photosynthetic reaction centers of different bacterial and plant species, revealing the ground-state electronic structures of the special pair (B)Chls [62]. The strong enhancement of the special-pair NMR signals owing to the CIDNP effect even allowed their detection in intact photosynthetic cells [67].

Methodological background of solid-state NMR

Introduction to solid-state NMR

The origin of NMR spectroscopy lies in studying the interactions between nuclear spins (I) and an external magnetic field (B_0). However, there are various external and intrinsic nuclear spin interactions either between nuclear spins and the external magnetic field, or among spins and the environment. A general Hamiltonian describing the NMR interaction is given by the following equation [68].

$$H = H_0 + H_{\mathrm{cs}} + H_{\mathrm{D}} + H_{\mathrm{J}} + \cdots , \qquad (1)$$

where H_0 stands for the Zeeman interaction, H_{cs} is the chemical shielding, H_{D} presents the dipolar coupling and H_{J} describes the scalar coupling.

The Zeeman interaction (the interaction between nuclear spin and external magnetic field) is given by

$$H_0 = -\gamma \hbar I . B_0 , \qquad (2)$$

where γ is the gyromagnetic ratio and B_0 the strength of external magnetic field. The Zeeman interaction is in the order of 10^7-10^9 Hz and it is the strongest interaction in NMR [69]. However the external magnetic field is not the same as the field that a nucleus locally feels. When atoms are placed in a strong external magnetic field, electrons start to circulate in their orbitals which results in the production of small local magnetic fields (B_{loc}) in order of few parts per million (ppm). Therefore, each nucleus experiences an effective magnetic field known as $B_{eff} = B_0 - B_{loc}$, which results in a change of the resonance frequency. The interaction of spins with a local magnetic field is known as chemical shielding and can be described as

$$H_{cs} = -\gamma\hbar\sigma I_z B_0 \ , \qquad (3)$$

where I_z is the z-component of the spin operator, and σ is the chemical shielding tensor and implies the anisotropic character of this interaction. Due to the fact that the charge distribution around a nucleus is rarely spherically symmetric a 3×3 matrix is used to describe the orientation dependence of the chemical shift or chemical shielding anisotropy (CSA) (for detailed information see [68]). In solid and solid like materials CSA results in a line broadening compared to materials dissolved in liquid.

The magnetic moments of two spins can be described as two magnetic bars interacting with each other. These interactions are several orders of magnitude smaller than the Zeeman interaction (10^3-10^5 Hz) and could be either through space or through bond. Through space interactions depend on the distance between two spins and are known as dipolar interactions and described by the following equation

$$H_D = H_{homo} + H_{hetero} \ , \qquad (4)$$

where H_{homo} is the dipolar interaction between the same type of nuclei and H_{hetero} stands for the interaction between the magnetic moments of two spins I and S. The corresponding quantum operator for homonuclear and heteronuclear dipolar interactions are given by

$$H_{hetero} = -\frac{\mu_0}{4\pi}\hbar\sum_i\sum_j \frac{\gamma^I\gamma^S}{r_{ij}^3}\frac{1}{2}(3cos^2\theta_{ij} - 1)2I_z^iS_z^j \ , \qquad (5)$$

$$H_{homo} = -\frac{\mu_0}{4\pi}\hbar\sum_i\sum_j \frac{\gamma^2}{r_{ij}^3}\frac{1}{2}(3cos^2\theta_{ij} - 1)(3I_z^iI_z^j - I^i.I^j) \ , \qquad (6)$$

where γ^i and γ^s are the gyromagnetic ratio of spin I and S, r_{ij} represents the internuclear distance between the nuclei i and j, θ_{ij} stands for the orientation of

the vector connecting two spins with respect to the external magnetic field and I_z^i and S_z^j are the z components of the nuclear spin of I and S [70] .

Through bond interactions known as scalar or J-couplings are small field independent interactions in the order of 1-10^3 Hz. the J-coupling is very sensitive to the changes in molecular structure, providing detailed structural information of the materials. Since these interactions are usually much smaller than the other interactions, they are often negligible in NMR spectra of solids. However, in solid like materials like membrane proteins, J-interactions play an important role that enable detection of mobile sites. The Hamiltonian for J-couplings is often given by

$$H_j = 2\pi\hbar J_{jk}\left(\vec{I_j}.\vec{I_k}\right), \tag{7}$$

where J_{jk} is the isotropic J-coupling.

Magic angle spinning (MAS)

In soluble materials, rapid molecular tumbling results in averaging the anisotropy and dipolar interactions and consequently sharp resonances are observed [68]. However for large protein complexes or solid materials, the molecular tumbling is significantly reduced leading to line broadening. In order to reduce the line width and spectral overlap in solid state NMR, Magic Angle Spinning (MAS) technique is employed. MAS NMR consists of spinning the sample at an angle θ_m with respect to the external magnetic field, by which anisotropic contributions to the dipolar and chemical anisotropy interactions that are scaled by the factor of $3cos^2\theta - 1$, become time dependent and are averaged to zero. As a result, a sharp peak can be observed while the angular dependent anisotropic contributions are spun away. Equation 8 defines the magic angle,

$$3cos^2\theta_{\mathrm{m}} - 1 = 0\,, \tag{8}$$

where $\theta_{\mathrm{m}} = 54.74$ is the angle with respect to the external magnetic field B_0.

The dynamic spectral-editing method

As mentioned in previous sections, the NMR sensitivity depends on the gyromagnetic ratio (γ) of the nucleus. Therefore, in order to detect nuclei with small gyromagnetic ratio, specific polarization transfer methods should be considered. In large systems, such as proteins, proton NMR results in spectral

crowding and ambiguous assignments. ^{13}C spectra with large spectral width of 200 ppm help to reduce spectral crowding, however due to the small γ_C which is ¼ of γ_H and low natural abundance of ^{13}C, ^{13}C NMR detection poses sensitivity problems.

The dynamic spectral-editing method consists of a combination of ^{13}C polarization-transfer solid-state NMR experiments. In ^{1}H-^{13}C polarization-transfer NMR, polarization is transferred from abundant ^{1}H nuclei with high gyromagnetic ratio (γ) to low sensitivity ^{13}C nuclei with low γ and the resulting ^{13}C spectrum is intensity enhanced, depending on the polarization-transfer efficiencies. The polarization transfer occurs via heteronuclear couplings between ^{13}C and ^{1}H nuclei, which are dipolar and scalar (*J*-) couplings. In cross polarization (CP)-based experiments [71], polarization is transferred via dipolar couplings. For mobile molecules, due to their fast random tumbling, dipolar couplings are averaged to zero within the contact time and consequently these components are filtered out from CP-based spectra. CP therefore acts as a dynamic filter that selectively probes rigid molecules. In INEPT-based experiments [72] polarization is transferred via *J*-couplings that are not affected by bond re-orientation. INEPT is effective if the transverse (T_2) relaxation times of the protons and carbons are sufficiently slow compared to the polarization transfer times. This is not the case for rigid molecules and therefore INEPT selectively probes mobile molecules [73]. With direct polarization (DP) [74], ^{13}C are directly excited by applying a 90° pulse to the ^{13}C carbons. DP provides a ^{13}C NMR spectrum of all molecular constituents. Figure 8 illustrates the efficiency of DP, INEPT and CP in different dynamics regimes.

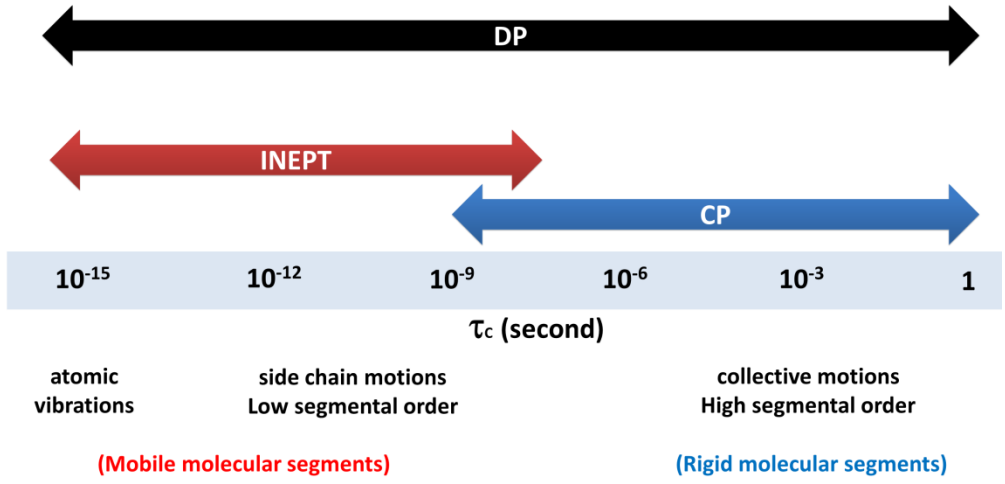

Figure 8. Schematic illustration of dynamic ranges where the DP, CP and INEPT pulse experiments are effective.

Cross polarization

In solid-state NMR, cross polarization (CP) is the building block of many pulse sequences. It was introduced in 1962 by Hartmann and Hahn for the static conditions. When a rare spin is in proximity of abundant nuclei, during a contact time polarization can be transferred from abundant nuclei to rare nuclei through strong heteronuclear couplings (see equation 5). In this method, after a 90^0 pulse, radio frequency pulses B_{1I} and B_{1S} are applied to different frequency channels, for instance ^{1}H and ^{13}C. For polarization transfer to occur, the nutation frequencies of the spin I and S must be identical and fulfil the Hartman-Hahn condition [75]. Equation 8 presents the Hartman-Hahn condition at static conditions.

$$|\omega_{1I}| = |\omega_{1S}| \,, \tag{9}$$

where $\omega_{1I} = -\gamma_{1I}B_{1I}$ and $\omega_{1S} = -\gamma_{1S}B_{1S}$.

The enhanced magnetization of the rare nuclei can hence be detected while the abundant nuclei are decoupled. The maximum enhancement of sensitivity is proportional to γ_{1I}/γ_{1S}. Figure 9 presents the schematics of the Hartman-Hahn condition and the basic pulse sequence of the CP experiment.

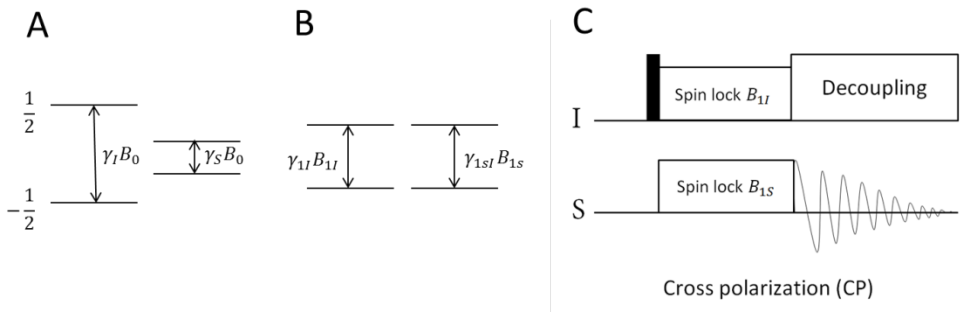

Figure 9. A: energy levels of spin I and S in the laboratory frame, **B:** energy levels of spin I and S in the rotating frame and C: basic pulse sequence of cross polarization between spin I and S.

Since the cross polarization (CP) occurs via dipolar couplings, it seems that under MAS conditions where dipolar couplings are averaged, CP must lose its efficiency. However, polarization transfer does occur as long as the coupling is not completely averaged, but becomes time dependent. In this condition CP is modified to the MAS version, where the B_1 of one of the contact pulses linearly increases or decreases in order to fulfil the Hartman-Hahn condition. In the

Hartman-Hahn condition under MAS the difference between the frequencies of two spins has to be a multiple of the spinning frequency and it is given by

$$\gamma_{1I}B_{1I} - \gamma_{1s}B_{1s=} \pm n\omega_r \ , \tag{10}$$

where n is an integer number [76-77].

Insensitive Nuclei Enhanced by Polarization Transfer

Another polarization transfer method is based on *J*-couplings (see equation 7) and known as Insensitive Nuclei Enhanced by Polarization Transfer or INEPT. INEPT is widely used in liquid NMR where *J*-couplings are strong enough for polarization transfer between nuclei. Although *J*-couplings are smaller compared to other interactions in solid materials, in biosolids such as membrane proteins, the INEPT sequences open a route to detect mobile species and get insight into their structure and dynamics. Figure 10 presents the pulse sequence of an INEPT experiment. The INEPT pulse sequence consists of several 90^0 and spin-echo pulses which lead to sensitivity enhancement of dilute nuclei. Like other NMR sequences INEPT starts with applying a 90^0 pulse to spin *I* to create transverse magnetization, followed by a time period delay for evolution of heteronuclear *J*-couplings. Furthermore spin echo pulses are applied to both nuclei in the middle of the evolution delay. The chemical shift of a spin *I* is refocused by a spin echo or 180^0 pulse in the *I* channel, while the heteronuclear *J*-couplings are not affected and a second delay is involved by only *I*-*S* couplings. As a result of spin echo pulses spin systems are in an antiphase state, this antiphase is converted to S nuclei and polarization is transferred from *I* to *S* by applying second 90^0 pulses on both channels. In order to create the in-phase x-magnetization, spin echo pulses are simultaneously applied to the *I* and *S* channels. Detailed steps of INEPT transfer by propagators are presented by equation 11 [78].

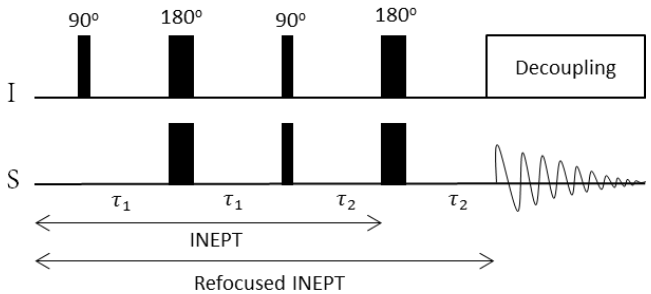

Figure 10. Pulse sequence of INEPT and refocused INEPT.

$$I_x \xrightarrow{2\pi J_{IS}\tau_1 I_z S_z} cos(2\pi J_{IS}\tau_1)\, I_x + sin(2\pi J_{IS}\tau_1) 2\, I_y S_z \qquad (11)$$

$$sin(2\pi J_{IS}\tau_1) 2\, I_y S_Z \xrightarrow{\left(\frac{\pi}{2}\right)_{I_x}} \xrightarrow{\left(\frac{\pi}{2}\right)_{S_x}} - sin(2\pi J_{IS}\tau_1) 2\, I_z S_y$$

$$\xrightarrow{2\pi J_{IS}\tau_2 I_z S_z} sin(2\pi J_{IS}\tau_2)\, sin(2\pi J_{IS}\tau_1)\, S_x\,.$$

Aim and scope of this thesis

This thesis aims to gain insight into the molecular mechanisms of light-harvesting regulation by addressing the conformational dynamics of light-harvesting complexes in native-like environments and the molecular dynamics of protein and lipid components in intact thylakoid membranes and whole cells.

The ability of MAS-NMR to study the *in-situ* conformational dynamics of light harvesting complexes at atomistic resolution in a native environment is demonstrated by employing polarization-transfer based dynamic filter experiments to isolated LHCII in lipid bilayers and intact thylakoid membranes.

Chapter 2 explains the applicability of solid-state NMR spectroscopy for obtaining a microscopic picture of different molecular constituents inside native thylakoid membranes. Moreover, the effect of Zea accumulation on dynamic properties of protein, lipid and xanthophyll constituents at physiological temperatures are discussed by comparing the dynamic-filter NMR spectra of *Cr.* thylakoid membranes from wild-type (WT) cells and from the *npq2* mutant that accumulates Zea.

Chapter 3 reveals that NMR signals of the most abundant light-harvesting complex, LHCII, can be detected in the spectra of native, heterogeneous thylakoid membranes. In order to investigate how the membrane environment influences on the dynamics and plasticity of LHCII, two-dimensional CP and INEPT based MAS-NMR experiments were performed on isolated *Cr.* LHCII reconstituted in lipid bilayers and on *Cr.* thylakoid membrane.

In **Chapter 4,** I describe the effect of Zea on the conformational dynamics of LHCII in a lipid bilayer. Hetero LHCII isolated from WT and *npq2 Cr.* cells were reconstituted in lipid bilayers and subjected to two-dimensional CP and INEPT based experiments.

Chapter 5 demonstrates how the dynamic spectra-editing NMR method that is introduced in chapter 2 can be extended to the cell level to resolve and quantify molecular dynamics of different cellular components. To this end, NMR experiments were applied on fresh, intact *Cr.* cells and results were compared with simulated CP and INEPT intensities.

Finally**,** a general discussion and perspectives of the research presented in this thesis is provided in **Chapter 6**.

References

1. Kromdijk, J.; Glowacka, K.; Leonelli, L.; Gabilly, S. T.; Iwai, M.; Niyogi, K. K.; Long, S. P., Improving photosynthesis and crop productivity by accelerating recovery from photoprotection. *Science (New York, N.Y.)* **2016,** *354* (6314), 857-861.
2. Harris, E., vhlamydomonas as a model system. *Annu. Rev. Plant Physiol. Plant Mol. Bio* **2001,** *52*, 363-406.
3. Blankenship, R. E., *Molecular mechanisms of photosynthesis*. Second edition ed.; Wiley/Blackwell: Chichester, West Sussex, 2014; p 296.
4. Croce, R.; van Amerongen, H., Light-harvesting in photosystem I. *Photosynth Res* **2013,** *116* (2-3), 153-66.
5. van Amerongen, H.; Croce, R., Light harvesting in photosystem II. *Photosynth Res* **2013,** *116* (2-3), 251-63.
6. Jordan, P.; Fromme, P.; Witt, H. T.; Klukas. O.; Saenger, W.; Krauss, N., Three-dimensional structure of cyanobacterial photosystem I at 2.5 Å resolution. *Nature* **2001,** *411*, 909-917.
7. Busch, A.; Hippler, M., The structure and function of eukaryotic photosystem I. *Biochim Biophys Acta* **2011,** *1807* (8), 864-77.
8. Ben-She1, A.; Frolow, F.; Nelson, N., Crystal structure of plant photosystem I. *Nature* **2003,** *426*, 630-635.
9. Amunts, A.; Toporik, H.; Borovikova, A.; Nelson, N., Structure determination and improved model of plant photosystem I. *J Biol Chem* **2010,** *285* (5), 3478-86.
10. Scheller, H. V.; Jenson, P. E.; Haldrup, A.; Lunde, C.; Knoetzel, J., Role of subunits in eukaryotic Photosystem I. *Biochimica et Biophysica Acta* **2001,** *1507*, 41-60.
11. Allen, J. F.; de Paula, W. B.; Puthiyaveetil, S.; Nield, J., A structural phylogenetic map for chloroplast photosynthesis. *Trends Plant Sci* **2011,** *16* (12), 645-55.
12. Mazor, Y.; Nataf, D.; Toporik, H.; Nelson, N., Crystal structures of virus-like photosystem I complexes from the mesophilic cyanobacterium Synechocystis PCC 6803. *Elife* **2013,** *3*, e01496.
13. Ganeteg, U.; Klimmek, F.; Jansson, S., Lhca5 – an LHC-type protein associated with photosystem I. *Plant Molecular Biology* **2004,** *54*, 641-651.
14. Elrad, D.; Grossman, A. R., A genome's-eye view of the light-harvesting polypeptides of *Chlamydomonas reinhardtii. Curr Genet* **2004,** *45* (2), 61-75.
15. Drop, B.; Webber-Birungi, M.; Fusetti, F.; Kouril, R.; Redding, K. E.; Boekema, E. J.; Croce, R., Photosystem I of *Chlamydomonas reinhardtii* contains nine light-harvesting complexes (Lhca) located on one side of the core. *J Biol Chem* **2011,** *286* (52), 44878-87.

16. Boekema, E. J.; Jenson, P. E.; Schlodder, E.; van Breemen, J. F. L.; van Roon, H.; Scheller, H. V.; Dekker, J. P., Green Plant Photosystem I Binds Light-Harvesting Complex I on One Side of the Complex. *Biochemistry* **2001,** *40*, 1029-1036.
17. Zouni, A.; Witt, H. T.; Kern, J.; Fromme, P.; Krauss, N.; Saenger, W.; Orth, P., Crystal structure of photosystem II from Synechococcuselongatusat 3.8 Å resolution. *Nature* **2001,** *409*, 739-743.
18. Umena, Y.; Kawakami, K.; Shen, J. R.; Kamiya, N., Crystal structure of oxygen-evolving photosystem II at a resolution of 1.9 A. *Nature* **2011,** *473* (7345), 55-60.
19. Guskov, A.; Kern, J.; Gabdulkhakov, A.; Broser, M.; Zouni, A.; Saenger, W., Cyanobacterial photosystem II at 2.9-A resolution and the role of quinones, lipids, channels and chloride. *Nat Struct Mol Biol* **2009,** *16* (3), 334-42.
20. Wei, X.; Su, X.; Cao, P.; Liu, X.; Chang, W.; Li, M.; Zhang, X.; Liu, Z., Structure of spinach photosystem II-LHCII supercomplex at 3.2 A resolution. *Nature* **2016,** *534* (7605), 69-74.
21. Pietrzykowska, M.; Pietrzykowska, M.; Suorsa, M.; Semchonok, D. A.; Tikkanen, M.; Boekema, E. J.; Jansson, S.; Jansson, S., The Light-Harvesting Chlorophyll a/b Binding Proteins Lhcb1 and Lhcb2 Play Complementary Roles during State Transitions in Arabidopsis. *Plant Cell* **2014,** *26* (9), 3646-3660.
22. Ferrante, P.; Ferrante, P.; Ballottari, M.; Bonente, G.; Giuliano, G.; Bassi, R., LHCBM1 and LHCBM2/7 Polypeptides, Components of Major LHCII Complex, Have Distinct Functional Roles in Photosynthetic Antenna System of *Chlamydomonas reinhardtii*. *Journal of biological chemistry* **2012,** *287* (20), 16276-16288.
23. Kulbrandt, W.; Wang, d. N.; Fojiyoshi, Y., Atomic model of plant light-harvesting complex by electron crystallography. *Nature* **1994,** *367*, 614-621.
24. Liu, Z.; Yan, H.; Wang, K.; Kuang, T.; Zhang, J.; Gui, L.; An, X.; Chang, W., Crystal structure of spinach major lightharvesting complex at 2.72A° resolution. *Nature* **2004,** *428*, 287-292.
25. Erickson, E.; Wakao, S.; Niyogi, K. K., Light stress and photoprotection in *Chlamydomonas reinhardtii*. *Plant J* **2015,** *82* (3), 449-65.
26. Kirchhoff, H., Structural changes of the thylakoid membrane network induced by high light stress in plant chloroplasts. *Philosophical Transactions of the Royal Society B: Biological Sciences* **2014,** *369* (1640), 20130225.
27. Horton, P.; Ruban, A., Molecular design of the photosystem II light-harvesting antenna: photosynthesis and photoprotection. *Journal of Experimental Botany* **2005,** *56* (411), 365-373.
28. Ruban, A.; Ruban, M.; Duffy, The photoprotective molecular switch in the photosystem II antenna. *Biochimica et biophysica acta. Bioenergetics* **2012,** *1817* (1), 167-181.
29. Müller, P.; L, X-P.; Niyogi, K. K., Non-Photochemical Quenching. A Response to Excess Light Energy1. *Plant Physiol 125*, 1558-1566.
30. Minagawa, J., State transitions--the molecular remodeling of photosynthetic supercomplexes that controls energy flow in the chloroplast. *Biochim Biophys Acta* **2011,** *1807* (8), 897-905.
31. Nilkens, M.; Kress, E.; Lambrev, P.; Miloslavina, Y.; Muller, M.; Holzwarth, A. R.; Jahns, P., Identification of a slowly inducible zeaxanthin-dependent component of non-photochemical quenching of chlorophyll fluorescence generated under steady-state conditions in Arabidopsis. *Biochim Biophys Acta* **2010,** *1797* (4), 466-75.
32. Krause, G. H., Photoinhibition of photosynthesis. An evaluation of damaging and protective mechanisms. *PHYSIOLOGIA PLANTARUM* **1988,** *74*, 566-574.
33. Lambrev, P. H.; Nilkens, M.; Miloslavina, Y.; Jahns, P.; Holzwarth, A. R., Kinetic and spectral resolution of multiple nonphotochemical quenching components in Arabidopsis leaves. *Plant Physiol* **2010,** *152* (3), 1611-24.
34. Xu, P.; Tian, L.; Kloz, M.; Croce, R., Molecular insights into Zeaxanthin-dependent quenching in higher plants. *Scientific Reports* **2015,** *5*, 13679.

35. Malnoë, A., Photoinhibition or photoprotection of photosynthesis? Update on the (newly termed) sustained quenching component qH. *Environmental and Experimental Botany* **2018**.
36. Li, X-P.; Muller-Mulle, P.; Gilmore, A. M.; Niyogi, K. K., PsbS-dependent enhancement of feedback de-excitation protects photosystem II from photoinhibition. *PNAS* **2016,** *113* (27).
37. Dinc, E.; Tian, L.; Roy, L. M.; Roth, R.; Goodenough, U.; Croce, R., LHCSR1 induces a fast and reversible pH-dependent fluorescence quenching in LHCII in *Chlamydomonas reinhardtii* cells. *Proc Natl Acad Sci U S A* **2016,** *113* (27), 7673-8.
38. Peers, G.; Truong, T. B.; Ostendorf, E.; Busch, A.; Elrad, D.; Grossman, A. R.; Hippler, M.; Niyogi, K. K., An ancient light-harvesting protein is critical for the regulation of algal photosynthesis. *Nature* **2009,** *462* (7272), 518-21.
39. Ballottari, M.; Alcocer, M. J.; D'Andrea, C.; Viola, D.; Ahn, T. K.; Petrozza, A.; Polli, D.; Fleming, G. R.; Cerullo, G.; Bassi, R., Regulation of photosystem I light harvesting by zeaxanthin. *Proc Natl Acad Sci U S A* **2014,** *111* (23), E2431-8.
40. Dall'Osto, L.; Cazzaniga, S.; Havaux, M.; Bassi, R., Enhanced photoprotection by protein-bound vs free xanthophyll pools: a comparative analysis of chlorophyll b and xanthophyll biosynthesis mutants. *Mol Plant* **2010,** *3* (3), 576-93.
41. Horton, P.; Ruban, A. V.; Wentworth, M., Allosteric regulation of the light-harvesting system of photosystem II. *Philos Trans R Soc Lond B Biol Sci* **2000,** *355* (1402), 1361-70.
42. Gruber, J. M.; Malý, P.; Krüger, T. P. J.; Grondelle, R. v., From isolated light-harvesting complexes to the thylakoid membrane: a single-molecule perspective. *Nanophotonics* **2018,** *7* (1), 81-92.
43. Park, S.; Fischer, A. L.; Steen, C. J.; Iwai, M.; Morris, J. M.; Walla, P. J.; Niyogi, K. K.; Fleming, G. R., Chlorophyll-Carotenoid Excitation Energy Transfer in High-Light-Exposed Thylakoid Membranes Investigated by Snapshot Transient Absorption Spectroscopy. *J Am Chem Soc* **2018,** *140* (38), 11965-11973.
44. Bode, S.; Quentmeier, C. C.; Liao, P-N.; Hafi, N.; Barros, T.; Wilk, W.; Bittner, F.; Walla, P. J, On the regulation of photosynthesis by excitonic interactions between carotenoids and chlorophylls. *PNAS* **2009,** *106*, 12311–12316.
45. Ruban, A. V.; Berera, R.; Ilioaia, C.; van Stokkum, I. H.; Kennis, J. T.; Pascal, A. A.; van Amerongen, H.; Robert, B.; Horton, P.; van Grondelle, R., Identification of a mechanism of photoprotective energy dissipation in higher plants. *Nature* **2007,** *450* (7169), 575-8.
46. Holt, N. E.; Zigmantas, D.; Valkunas, L.; Li, X.; Niyogi, K.; Fleming, G. R., Carotenoid Cation Formation and the Regulation of Photosynthetic Light Harvesting. *Science* **2005,** *307*, 433-436.
47. Barros, T.; Royant, A.; Standfuss, J.; Dreuw, A.; Kuhlbrandt, W., Crystal structure of plant light-harvesting complex shows the active, energy-transmitting state. *EMBO J* **2009,** *28* (3), 298-306.
48. Higman, V. A.; Varga, K.; Aslimovska, L.; Judge, P. J.; Sperling, L. J.; Rienstra, C. M.; Watts, A., The Conformation of Bacteriorhodopsin Loops in Purple Membranes Resolved by Solid-State MAS NMR Spectroscopy. *Angewandte Chemie International Edition* **2011,** *50* (36), 8432-8435.
49. Kulminskaya, N. V.; Pedersen, M. Ø.; Bjerring, M.; Underhaug, J.; Miller, M.; Frigaard, N.-U.; Nielsen, J. T.; Nielsen, N. C., In Situ Solid-State NMR Spectroscopy of Protein in Heterogeneous Membranes: The Baseplate Antenna Complex of Chlorobaculum tepidum. *Angewandte Chemie International Edition* **2012,** *51* (28), 6891-6895.
50. Kaplan, M.; Cukkemane, A.; van Zundert, G. C.; Narasimhan, S.; Daniels, M.; Mance, D.; Waksman, G.; Bonvin, A. M.; Fronzes, R.; Folkers, G. E.; Baldus, M., Probing a cell-embedded megadalton protein complex by DNP-supported solid-state NMR. *Nature methods* **2015,** *12* (7), 649-52.

51. Kaplan, M.; Narasimhan, S.; de Heus, C.; Mance, D.; van Doorn, S.; Houben, K.; Popov-Celeketic, D.; Damman, R.; Katrukha, E. A.; Jain, P.; Geerts, W. J. C.; Heck, A. J. R.; Folkers, G. E.; Kapitein, L. C.; Lemeer, S.; van Bergen En Henegouwen, P. M. P.; Baldus, M., EGFR Dynamics Change during Activation in Native Membranes as Revealed by NMR. *Cell* **2016,** *167* (5), 1241-1251 e11.
52. Pinto, C.; Mance, D.; Julien, M.; Daniels, M.; Weingarth, M.; Baldus, M., Studying assembly of the BAM complex in native membranes by cellular solid-state NMR spectroscopy. *Journal of structural biology* **2017**.
53. Baker, L. A.; Sinnige, T.; Schellenberger, P.; de Keyzer, J.; Siebert, C. A.; Driessen, A. J. M.; Baldus, M.; Grunewald, K., Combined (1)H-Detected Solid-State NMR Spectroscopy and Electron Cryotomography to Study Membrane Proteins across Resolutions in Native Environments. *Structure (London, England : 1993)* **2017**.
54. Ward, M. E.; Wang, S.; Munro, R.; Ritz, E.; Hung, I.; Gor'kov, Peter L.; Jiang, Y.; Liang, H.; Brown, Leonid S.; Ladizhansky, V., In Situ Structural Studies of Anabaena Sensory Rhodopsin in the E. coli Membrane. *Biophysical Journal* **2015,** *108* (7), 1683-1696.
55. Fu, R.; Wang, X.; Li, C.; Santiago-Miranda, A. N.; Pielak, G. J.; Tian, F., In situ structural characterization of a recombinant protein in native Escherichia coli membranes with solid-state magic-angle-spinning NMR. *Journal of the American Chemical Society* **2011,** *133* (32), 12370-3.
56. Miao, Y.; Qin, H.; Fu, R.; Sharma, M.; Can, T.; Hung, I.; Luca, S.; Gor'kov, P. L.; Brey, W. W.; Cross, T. A., M2 Proton Channel Structural Validation from Full Length Protein Samples in Synthetic Bilayers and E. coli Membranes. *Angewandte Chemie (International ed. in English)* **2012,** *51* (33), 8383-8386.
57. Renault, M.; Pawsey, S.; Bos, M. P.; Koers, E. J.; Nand, D.; Tommassen-van Boxtel, R.; Rosay, M.; Tommassen, J.; Maas, W. E.; Baldus, M., Solid-state NMR spectroscopy on cellular preparations enhanced by dynamic nuclear polarization. *Angew Chem Int Ed Engl* **2012,** *51* (12), 2998-3001.
58. Jacso, T.; Franks, W. T.; Rose, H.; Fink, U.; Broecker, J.; Keller, S.; Oschkinat, H.; Reif, B., Characterization of membrane proteins in isolated native cellular membranes by dynamic nuclear polarization solid-state NMR spectroscopy without purification and reconstitution. *Angew Chem Int Ed Engl* **2012,** *51* (2), 432-5.
59. Bill, R. M.; Henderson, P. J.; Iwata, S.; Kunji, E. R.; Michel, H.; Neutze, R.; Newstead, S.; Poolman, B.; Tate, C. G.; Vogel, H., Overcoming barriers to membrane protein structure determination. *Nat Biotechnol* **2011,** *29* (4), 335-40.
60. Stroud, R. M., New tools in membrane protein determination. *F1000 Biol. Rep* **2011,** *3* (8).
61. Wang, S.; Munro, R. A.; Shi, L.; Kawamura, I.; Okitsu, T.; Wada, A.; Kim, S. Y.; Jung, K. H.; Brown, L. S.; Ladizhansky, V., Solid-state NMR spectroscopy structure determination of a lipid-embedded heptahelical membrane protein. *Nat Methods* **2013,** *10* (10), 1007-12.
62. Alia, A.; Buda, F.; de Groot, H. J.; Matysik, J., Solid-state NMR of nanomachines involved in photosynthetic energy conversion. *Annu Rev Biophys* **2013,** *42*, 675-99.
63. Pandit, A.; de Groot, H. J., Solid-state NMR applied to photosynthetic light-harvesting complexes. *Photosynth Res* **2012,** *111* (1-2), 219-26.
64. Sunku, K.; de Groot, H. J.; Pandit, A., Insights into the photoprotective switch of the major light-harvesting complex II (LHCII): a preserved core of arginine-glutamate interlocked helices complemented by adjustable loops. *J Biol Chem* **2013,** *288* (27), 19796-804.
65. Pandit, A.; Reus, M.; Morosinotto, T.; Bassi, R.; Holzwarth, A.; Holzwarth, A. R., An NMR comparison of the light-harvesting complex II (LHCII) in active and photoprotective states reveals subtle changes in the chlorophyll a ground-state electronic structures. *Biochimica et biophysica acta. Bioenergetics* **2013,** *1827* (6), 738-744.

66. Duffy, C. D.; Pandit, A.; Ruban, A. V., Modeling the NMR signatures associated with the functional conformational switch in the major light-harvesting antenna of photosystem II in higher plants. *Phys Chem Chem Phys* **2014,** *16* (12), 5571-80.
67. Prakash, A. S.; Gast, P.; de Groot, H. J.; Matysik, J.; Jeschke, G., Photo-CIDNP MAS NMR in Intact Cells of Rhodobacter sphaeroides R26: Molecular and Atomic Resolution at Nanomolar Concentration. *Journal of the American Chemical Society* **2008,** *128*.68. Duer, M. J., *Solid-State NMR Spectroscopy Principles and Applications*. 2002.
69. Smith, M. E.; Mackenzie. E., *Multinuclear Solid-State Nuclear Magnetic Resonance of Inorganic Materials*. 1th ed.; 2002.
70. Schmidt-Rohr, K.; Spiess. W., Multidimentional Solid-State NMR and Polymers. *Academic Press Ltd., London* **1994**.
71. Pines, A.; Waugh J. S.; Gibby, M. G., Proton-Enhanced Nuclear Induction Spectroscopy - Method for High-Resolution Nmr of Dilute Spins in Solids. *The Journal of Chemical Physics* **1972,** *56* (4), 1776.
72. Morris, G. A.; Freeman, R., Enhancement of nuclear magnetic resonance signals by polarization transfer. *J. Am. Chem. Soc* **1979,** *101* (3), 760–762.
73. Nowacka, A.; Mohr, P. C.; Norrman, J.; Martin, R. W.; Topgaard, D., Polarization transfer solid-state NMR for studying surfactant phase behavior. *Langmuir* **2010,** *26* (22), 16848-56.
74. Purusottam, R. N.; Bodenhausen, G.; Tekely, P., Quantitative one- and two-dimensional 13C spectra of microcrystalline proteins with enhanced intensity. *J Biomol NMR* **2013,** *57* (1), 11-9.
75. Hartmann, S. R.; Hahn, E. L., Nuclear Double Resonance in the Rotating Frame. *Physical Review* **1962,** *128* (5), 2042-2053.
76. Stejskal, E.; Schaefer, J.; Waugh, J., Magic-angle spinning and polarization transfer in proton-enhanced NMR. *J. Magn. Reson* **1977,** *28*, 105–112.
77. Pines, A.; Gibby, M. G.; Waugh, J. S., Proton-enhanced NMR of dilute spins in solids. *The Journal of Chemical Physics* **1973,** *69* (2), 569-590.
78. Morris, G. A.; Freeman, R., Enhancement of nuclear magnetic resonance signals by polarization transfer. *J. Am. Chem. Soc* **1979,** *101* (3), 760–762.